Received: 23 March 2017 | Revised: 21 December 2017 | Accepted: 23 August 2018 | Published on: 17 December 2018

DOI: 10.1002/met.1761

Meteorological Applications RMetS

RESEARCH ARTICLE

Investigation of various aerosols over different locations in South Africa using satellite, model simulations and LIDAR

Lerato Shikwambana[1,2] | Venkataraman Sivakumar[1]

[1]School of Chemistry and Physics, University of KwaZulu-Natal, Durban, South Africa

[2]Space Science Division, South African National Space Agency, Hermanus, South Africa

Correspondence
Lerato Shikwambana, Space Science Division, South African National Space Agency, Hermanus, South Africa.
Email: lshikwambana@gmail.com

Decadal studies (2004–2014) of various aerosols were carried out over South Africa (SA) using various satellite data and model simulations. The aerosols investigated included black carbon (BC), sulphate, dust and marine aerosols. BC aerosols were observed to be dominant in the northeastern parts of SA while sulphate aerosols were dominant in eastern parts of the country. Seasonal studies revealed that BC aerosols were more dominant in the eastern parts of SA during spring and less dominant in autumn. Sulphate also showed dominance in the eastern parts of SA during summer and less dominance in winter. The high sulphate concentration in summer is a result of an increase in relative humidity which favours the production of sulphates. Air masses from the north and northeastern parts of the subcontinent were responsible for the transport of BC resulting from biomass burning into SA. The Goddard Chemistry Aerosol Radiation and Transport model indicated that there was no significant change in the sulphate aerosol trends from 2004 to 2007. The highest sulphate aerosol levels were observed in the summer whilst the lowest sulphate aerosol levels were observed in winter. The Council for Scientific and Industrial Research (CSIR) Light Detection and Ranging (LIDAR) was used to carry out measurements in Lephalale during July 10–18, 2014. Aerosol extinction co-efficient profiles were retrieved by the CSIR mobile LIDAR and were compared to aerosol extinction co-efficient profiles retrieved from the Cloud-Aerosol LIDAR and Infrared Pathfinder Satellite Observations (CALIPSO). The aerosol extinction co-efficients of 0.26 and 0.17/km on July 14 and 16, 2014, respectively could be identified as dust aerosols.

KEYWORDS
aerosols, AOD, LIDAR, MERRA-2

1 | INTRODUCTION

In the past air pollution has been widely discussed primarily because of its health and environmental effects. Chemical emissions from factories, dust, pollen and emissions from vehicles may be suspended as particles in the atmosphere, thus contributing to air pollution. Black carbon (BC) aerosols are produced from anthropogenic and natural activities and are known to absorb visible and infrared radiation which may lead to atmospheric warming (Ahmed *et al*., 2014; Kompalli *et al*., 2014; Panicker *et al*., 2014; Zhang *et al*., 2015). Sulphate aerosols have both natural and anthropogenic sources. Natural sources include volcanic eruptions and marine emissions (Ray and Kim, 2014) whilst biomass burning, industrial combustion and coal burning are some anthropogenic activities responsible for the emission of sulphate. Sulphates are known to cause cooling in the atmosphere by scattering incoming radiation (Seinfeld and Pandis, 2006). Dust has also been reported to modify the atmospheric radiative budget by absorbing and scattering solar radiation. Dust can be easily transported over large distances from its source region making it a potential source for long range transport of bacteria (Ginoux *et al*., 2004). More recently Tesfaye *et al*. (2015) showed that the desert dust

particles which load the western and southern regions of South Africa (SA) originate mainly from the Kalahari and Namib Desert areas.

A number of aerosol studies have been carried out in Southern Africa (Piketh *et al*., 1999; Queface *et al*., 2001; Ross *et al*., 2003; Magi, 2009; Kumar *et al*., 2014; Hersey *et al*., 2015; Kuik *et al*., 2015; Kneen *et al*., 2016). Over and above this the Southern African Regional Science Initiative (SAFARI 2000) project was carried out over a 2 year period from March 1999 to March 2001. The main objectives were (a) to characterize, quantify and understand the processes driving biogenic, pyrogenic and anthropogenic emissions in southern Africa, with particular attention paid to atmospheric transport, chemical transformation and deposition, (b) to validate the remote sensing data obtained from the Terra satellite of terrestrial and atmospheric processes and (c) to study the influence of aerosol and trace gases on the radiation budget through their modification of the optical and microphysical properties of clouds (Swap *et al*., 2003). Several studies were conducted and several papers were published during this campaign (Campbell *et al*., 2003; Eck *et al*., 2003; Formenti *et al*., 2003; Swap *et al*., 2003; Winkler *et al*., 2008).

In the present study the Modern-Era Retrospective Analysis for Research and Applications, Version 2 (MERRA-2) (from 2004 to 2014) was used to study BC, sulphate, dust and sea-salt extinction aerosol optical depth (AOD) in SA. It is believed that the study using MERRA-2 data over SA has not been previously performed. Selected sites for a part of this study include Lephalale (23.6665 ° S, 27.7448 ° E), Bloemhof (27.6263 ° S, 25.5800 ° E), Mafikeng (25.8560 ° S, 25.6403 ° E), Potchefstroom (26.7145 ° S, 27.0970 ° E), Rustenburg (25.6544 ° S, 27.2559 ° E) and Vryburg (26.9584 ° S, 24.7299 ° E). These are all towns known to have a high rate of mining and industrial activities which would result in high aerosol loading.

The first objective of the work was to study a 10 year and seasonal climatology of BC, sulphate, dust and marine aerosols in SA using MERRA-2. The MERRA-2 data were validated against the Aerosol Robotic Network (AERONET) data. The second objective of the work was to study the climatology of BC, sulphate and dust in the towns of Lephalale, Bloemhof, Mafikeng, Potchefstroom, Rustenburg and Vryburg using the Goddard Chemistry Aerosol Radiation and Transport (GOCART) model. The third objective was to study the vertical profiles of aerosol extinction co-efficients in Lephalale using the Council for Scientific and Industrial Research (CSIR) mobile Light Detection and Ranging (LIDAR) and Cloud-Aerosol LIDAR and Infrared Pathfinder Satellite Observations (CALIPSO). It should be noted that LIDAR measurements were only carried out in Lephalale. The selection of this study site was motivated by the mining and industrial activities that occur in that area.

2 | CASE STUDY LOCATIONS

Limpopo and the northwest provinces in SA (Figure 1) were selected for this study because of their different geographical and climatological characteristics as well as economic activities that might contribute to aerosol loading in these regions. Lephalale is a small developing town in the Limpopo province with mining, agriculture and electricity production activities. The selection of the towns in the northwest province was motivated by a study conducted by Aurela *et al*. (2016) in the northwest province and its surroundings. Aurela *et al*. (2016) described the site as a dry savannah regional background site, with no major local anthropogenic sources. They showed that the surroundings contained

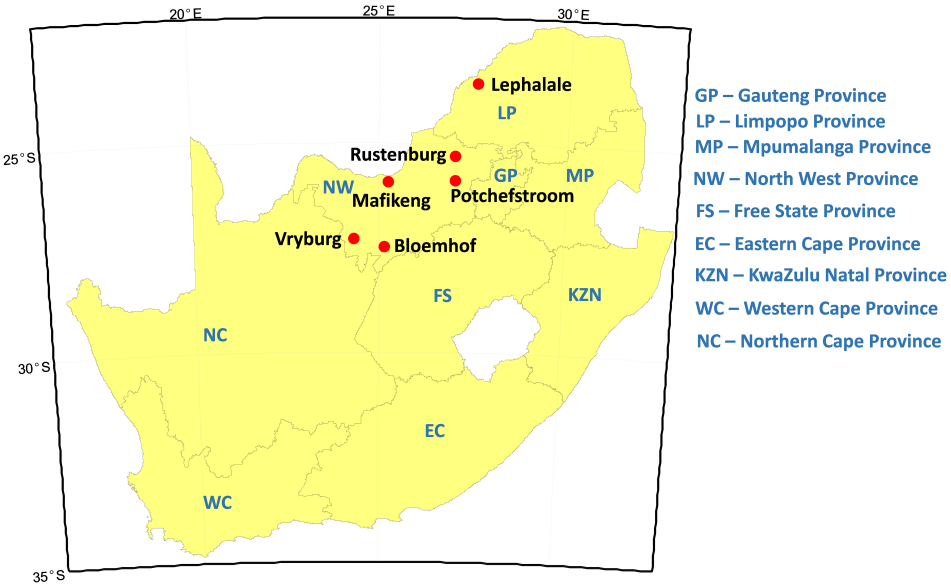

FIGURE 1 A map of South Africa showing the nine provinces with towns where studies were conducted [Colour figure can be viewed at wileyonlinelibrary.com]

several large anthropogenic sources from mining and pyrometallurgical smelting activities. In this work certain aerosol characterizations were performed using a specific model for selected individual towns. Bloemhof and Mafikeng are small towns in the northwest province with industrial activities whereas Potchefstroom and Vryburg have predominately farming activities. Rustenburg is characterized by a large number of facilities connected to the mining industry. It should be mentioned that LIDAR and CALIPSO measurements were only carried out in Lephalale and not in the other towns. However, the GOCART model data are discussed for all the towns.

3 | METHOD AND DATA

3.1 | Modern-Era Retrospective Analysis for Research and Applications, Version 2 (MERRA-2)

MERRA-2 is a NASA reanalysis product using a major new version of the Goddard Earth Observing System Data Assimilation System Version 5 (GEOS-5) (https://gmao.gsfc.nasa.gov/reanalysis/MERRA-2/). The Global Modeling and Assimilation Office has used its GEOS-5 atmospheric data assimilation system to synthesize the various observations collected over the satellite era (from 1980 to the present) into a dataset that is as consistent as possible over time as it uses a fixed assimilation system. MERRA is being conducted with version 5.2.0 of the GEOS-5 atmospheric data assimilation system with a 0.5 ° latitude × 0.625 ° longitude × 72 layer model configuration (Rienecker *et al*., 2011). MERRA-2 assimilates bias-corrected AOD from the Moderate Resolution Imaging Spectroradiometer (MODIS) and the Advanced Very High Resolution Radiometer instruments (Buchard *et al*., 2017; Randles *et al*., 2017). Buchard *et al*. (2017) showed that the assimilated AOD observations do not constrain aerosol speciation, absorption properties or aerosol vertical structure; the data assimilation system does produce diagnostics of these unconstrained quantities. They further showed that the accuracy of MERRA-2 aerosol diagnostics depends not only on the quality of AOD observed and the data assimilation algorithm, but also on the quality of the background or forecast model. In this work MERRA-2 was used to produce 3D fields of BC, sulphate, dust and sea-salt over the period 2004–2014.

3.2 | Goddard Chemistry Aerosol Radiation and Transport (GOCART) model

The GOCART model simulates major tropospheric aerosol components such as sulphates, dust and BC. It has the same horizontal resolution as the Goddard Earth Observing System Data Assimilation System (GEOS DAS), 2 ° latitude × 2.5 ° longitude and 20–30 vertical sigma layers, and uses the assimilated meteorological fields generated from GEOS DAS (Chin *et al*., 2001; Ginoux *et al*., 2001). A detailed description of the model is given by Chin *et al*. (2000). In this study, the climatology of BC, sulphate and dust over the period 2004–2007 was investigated.

3.3 | Moderate Resolution Imaging Spectroradiometer (MODIS)

The MODIS views a 2,300 km wide swath, from a polar orbit of 700 km, providing near daily coverage of Earth's surface and atmosphere (Cheng *et al*., 2012). The MODIS measures radiance in 36 channels spanning the spectral range 0.44–15 μm, with a varying spatial resolution of 250 m (bands 1 and 2), 500 m (bands 3–7) and 1 km (bands 8–36). A detailed description and operation of the Terra MODIS has been described by several authors (Kaskaoutis *et al*., 2006; Baddock *et al*., 2009; El-Metwally *et al*., 2010). In this study, monthly mean level 3 products from the Terra MODIS (MOD08M3.051) were used for the period 2004–2014.

3.4 | Multi-angle Imaging Spectroradiometer (MISR)

The MISR provides ongoing global coverage with high spatial resolution. It uses nine cameras pointed at fixed angles, one viewing the nadir direction and four each viewing the forward and backward directions along the spacecraft ground track. Information on the MSIR technical specifications is described by Diner *et al*. (1998). The MISR data products are grouped into three levels of processing. Level 3 processing will produce data aggregated over various time scales (monthly, seasonally, annually) on a global map grid. For this study, the monthly MISR level 3 data global 0.5 ° × 0.5 ° aerosol product was used for the period January 2004 to December 2014.

3.5 | CSIR mobile LIDAR

The Mie LIDAR system at the CSIR, in Pretoria (25.7461 ° S, 28.1881 ° E), was developed in 2007. This LIDAR has been configured into mono-static that maximizes the overlap of the outgoing beam with the receiver field of view. The LIDAR system has been mounted in a mobile platform with a special shock absorber frame (Sharma *et al*., 2009; Sivakumar *et al*., 2009). Sharma *et al*. (2009) have given a more detailed description of the CSIR National Laser Centre mobile LIDAR system. More recent work by Shikwambana and Sivakumar (2016) address the scientific results obtained and data analysis. LIDAR measurements were carried out only during the day from July 11 to 18, 2014, in Lephalale (23.6665 ° S, 27.7448 ° E). The backscatter signals were collected and their intensities were measured. The Klett method was then used to calculate the aerosol backscatter co-efficients and the aerosol extinction co-efficients.

TABLE 1 Summary of the data used in this study

Input data source (temporal resolution, spatial resolution) (latitude; longitude)	Products used	Period of analysis	Output data
MERRA-2 model (monthly; 0.5 ° × 0.625 °) RSA (14.5 °, 35.4 °; −34.8 °, −22.2 °)	BC AOD (550 nm)	2004–2014	10 year mean climatology of BC AOD
	Sulphate AOD (550 nm)		10 year mean climatology of sulphate AOD
	Dust AOD (550 nm)		10 year mean climatology of dust AOD
	Marine AOD (550 nm)		10 year mean climatology of marine AOD
Terra MODIS (monthly, 1 °) RSA (14.5 °, 35.4 °; −34.8 °, −22.2 °)	AOD (550 nm)	2004–2014	Mean AOD climatology for South Africa
MISR (monthly, 0.5 °) RSA (14.5 °, 35.4 °; −34.8 °, −22.2 °)	AOD (555 nm)	2004–2014	Mean AOD climatology for South Africa
GOCART (monthly, 2 ° × 2.5 °)	BC AOD	2004–2007	BC AOD trend from 2004 to 2007
Lephalale (23.6665 ° S, 27.7448 ° E) Bloemhof (27.6263 ° S, 25.5800 ° E), Mafikeng (25.8560 ° S, 25.640 3° E), Potchefstroom (26.7145 ° S, 27.0970 ° E) Rustenburg (25.6544 ° S, 27.2559 ° E) Vryburg (26.9584 ° S, 24.7299 ° E)	Sulphate AOD		Sulphate AOD trend from 2004 to 2007
	Dust AOD		Dust AOD trend from 2004 to 2007
CSIR mobile LIDAR (daily) Lephalale (23.6665 ° S, 27.7448 ° E)	LIDAR backscatter signal returns	July 10–18, 2014	Aerosol extinction co-efficient (/km) profiles
CALIPSO (5.92 s, 5 km) Lephalale (23.6665 ° S, 27.7448 ° E)	Aerosol profile	July 12, 13, 14 and 16, 2014	Aerosol extinction co-efficient (/km) profiles
AERONET Pretoria (25.75 ° S, 28.23 ° E)	Level 2.0 $AOD_{500\ nm}$ (quality assured)	August–December 2010	Averaged monthly AOD

AERONET, Aerosol Robotic Network; AOD, aerosol optical depth; BC, black carbon; CALIPSO, Cloud-Aerosol LIDAR and Infrared Pathfinder Satellite Observations; CSIR, Council for Scientific and Industrial Research; GOCART, Goddard Chemistry Aerosol Radiation and Transport; LIDAR, Light Detection and Ranging; MERRA-2, Modern-Era Retrospective Analysis for Research and Applications, Version 2; MISR, Multi-angle Imaging Spectroradiometer; MODIS, Moderate Resolution Imaging Spectroradiometer.

3.6 | Cloud-Aerosol LIDAR and Infrared Pathfinder Satellite Observations (CALIPSO)

The CALIPSO provide information about the thickness of clouds and can determine the height and types of aerosols. The CALIPSO satellite consists of three co-aligned nadir-viewing instruments: the Cloud-Aerosol LIDAR with Orthogonal Polarization (CALIOP), an imaging infrared radiometer and a wide field camera. CALIOP is a sensitive LIDAR that provides high-resolution vertical profiles of aerosols and clouds. CALIOP products can be separated into two levels: (a) level 1 products are composed of calibrated and geo-located profiles of the attenuated backscatter returned signal and (b) level 2 products are derived from level 1 products and are classified in three types: layer products, profile products and vertical feature mask (Lopes *et al*., 2012).

A summary of the input and output data for each method used for the present study is given in Table 1.

4 | RESULTS AND DISCUSSION

4.1 | Validation of the MERRA-2 model

The seasonal AODs retrieved by the MERRA-2 model in Pretoria (25.75 ° S, 28.23 ° E) from July 2011 to December 2014 are shown in Figure 2. They were compared with the measured satellite AOD data from the MODIS and the ground based AOD data from the AERONET station based at the CSIR in Pretoria. For the 2011–2012 period all three instruments showed an increase in AOD from the winter (June, July, August) to the summer (December, January, February). After the summer there was a decrease in the AOD values in the autumn (March, April, May). A high AOD observed during the summer could be a result of biomass burning activities in southern Africa. The AERONET always showed the highest AOD values compared to the MODIS and the MERRA-2 during the study period. This may be due to the good temporal resolution of the instrument and better averaging of the data. The Terra MODIS overpasses the study region once a day resulting in a poor temporal resolution. In most instances AOD retrieved by

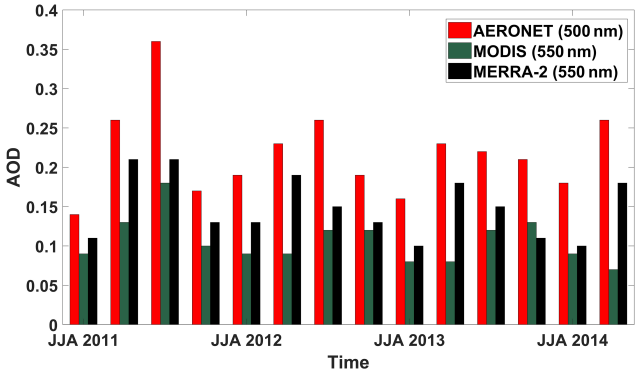

FIGURE 2 Comparison of aerosol optical depth (AOD) using the Aerosol Robotic Network (AERONET), the Moderate Resolution Imaging Spectroradiometer (MODIS) and the Modern-Era Retrospective Analysis for Research and Applications, Version 2 (MERRA-2) data [Colour figure can be viewed at wileyonlinelibrary.com]

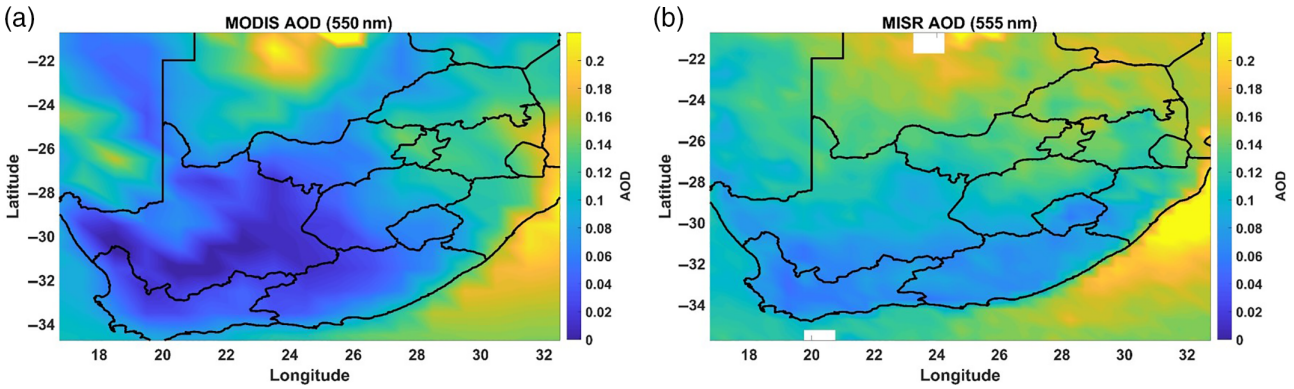

FIGURE 3 Latitude–longitude colour map of mean aerosol optical depth (AOD) for South Africa using (a) the Moderate Resolution Imaging Spectroradiometer (MODIS) (550 nm) and (b) the Multi-angle Imaging Spectroradiometer (MISR) (555 nm) [Colour figure can be viewed at wileyonlinelibrary.com]

MERRA-2 is more comparable to AERONET AOD than MODIS AOD. The MODIS AOD observations were found to be biased.

4.2 | Spatial distributions of AOD using the MODIS and MISR

The averaged $AOD_{550\ nm}$ and $AOD_{555\ nm}$ in SA for the period 2004–2014 using the MODIS and MISR are shown in Figure 3a,b respectively. The averaged AOD retrieved from the databases of both instruments shows a high aerosol loading in the northern and eastern parts of the country, namely the Limpopo and Mpumalanga provinces. The east coast of SA also exhibits high aerosol loading. A low aerosol loading is observed in the southern parts of SA as measured by both instruments. The MODIS AOD in the northern parts of SA is observed as ~0.11 whereas the MISR AOD for the northern parts is observed as ~0.16. The MODIS results agree with earlier research by Kumar *et al*. (2014) and Hersey *et al*. (2015). However, it is observed that the MISR gives slightly higher AOD compared to the MODIS. This is also observed in the southern parts of SA were the MODIS AOD is ~0.02 and the MISR AOD is ~0.08. Discrepancies in AOD between satellite platforms are generally within uncertainty and the differences in AOD values might be due to calibration and retrieval algorithms, processing methods, the complex surface (Guo *et al*., 2014) and the overpass time of the satellites over SA (Hersey *et al*., 2015). Other factors that might contribute to the differences include the difference in spatial resolution and swath dimension of these instruments.

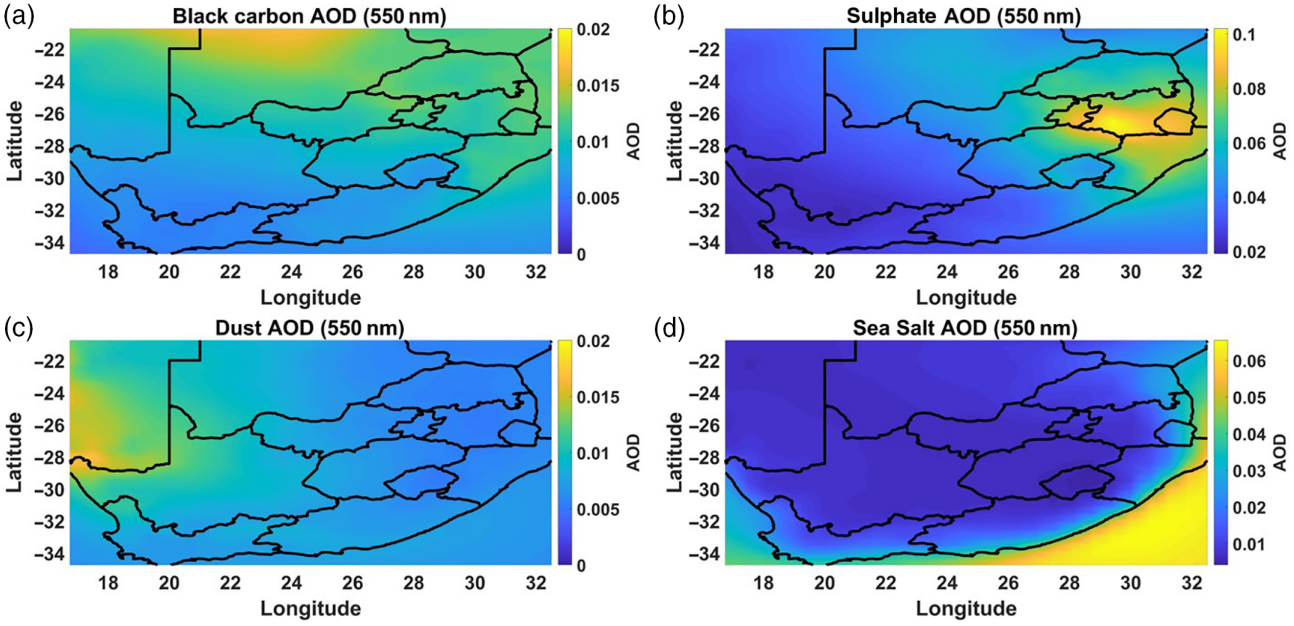

FIGURE 4 Spatial distribution of (a) black carbon aerosol optical depth (AOD) (550 nm), (b) sulphate AOD (550 nm), (c) dust AOD (550 nm) and (d) sea-salt AOD (550 nm) as derived from the Modern-Era Retrospective Analysis for Research and Applications, Version 2 (MERRA-2) for a period of 10 years (2004–2014) [Colour figure can be viewed at wileyonlinelibrary.com]

4.3 | BC, sulphate, dust and marine AOD observed by the MERRA-2

The spatial distributions of aerosols for SA averaged from 2004 to 2014 and retrieved by MERRA-2 are shown in Figure 4. BC aerosols are dominant in the northeastern parts of SA (see Figure 4a). This dominance can also be observed on the borders of the neighbouring countries, i.e. Botswana, Zimbabwe and Mozambique, and corresponds to a BC AOD of ~0.014. In general, the biggest contributors of BC aerosols are from incomplete combustion processes such as fossil fuel and biomass burning. The southern Africa regional biomass burning occurs from June to October (Cooke and Wilson, 1996). Cahoon *et al*. (1992) showed that air masses from the north and northeastern parts of the subcontinent transport a substantial amount of pollution resulting from biomass burning. From the SAFARI 2000 campaign biomass burning smoke and haze from central Africa were observed exiting off the east coast of SA on September 4, 2000 (Swap *et al*., 2003). The SAFARI 2000 campaign showed that the transported biomass burning smoke enhanced the AOD in SA during the August and September period (Eck *et al*., 2003; Formenti *et al*., 2003) and the impact in SA originates in neighbouring countries such as Zimbabwe and Mozambique (Magi *et al*., 2009). By comparison lower aerosol loading (AOD ~ 0.005) of BC is observed in the southwestern parts of SA and this extends to the Atlantic Ocean. However, the mid-latitude of SA is dominated by moderate BC (AOD ~ 0.008).

Sulphate aerosols are mostly concentrated in the eastern parts of SA in Mpumalanga province (see Figure 4b) with elevated aerosol loading (AOD ~ 0.1). Swaziland also showed elevated sulphate aerosol loading (AOD ~ 0.085). Some of the northern and southeastern parts of SA have moderate sulphate loading corresponding to AOD ~ 0.07. The elevated and moderate sulphate aerosols are from the industrial activities in the Highveld and pyrometallurgical processing of copper in the Democratic Republic of Congo and the Zambian copper belt as reported by Piketh *et al*. (1999), Zunckel *et al*. (2000) and Freiman and Piketh (2003). Coal combustion for power production might also be a major contributor to the elevated sulphate aerosol loading in the Mpumalanga region. The Mpumalanga province has 11 operational coal fired power stations which are a source for most of the sulphates in the region. A lower sulphate aerosol loading (AOD ~ 0.03) is observed from the central interior to the southwestern part of SA. This finding is supported by Tesfaye *et al*. (2014) using the Regional Climate Model (RegCM4). It is also known that sulphate aerosols can be produced within the atmosphere by oxidation of reduced sulfur species such as dimethyl sulfide emitted by oceanic phytoplankton (Alexander *et al*., 2005). Since the western parts of SA have low industrial activities and biomass burning, the major contribution of the sulphate could arise from emitted dimethyl sulfide. However, deliquescent sea-salt and dust aerosols have also been reported to be possible sites for aqueous phase sulphate production (Alexander *et al*., 2005).

Dust aerosols are more dominant in the northwestern parts of SA (see Figure 4c) where an elevated dust aerosol loading (AOD ~ 0.013) is observed near the border of Namibia. This dust aerosol loading is produced in the Kalahari and Namib Desert areas (Tesfaye *et al*., 2015). A lower dust aerosol loading (AOD ~ 0.006) is observed in the northern, eastern and southeastern parts of SA. The interior of the country shows a moderate dust aerosol loading (AOD ~ 0.009).

Sea-salt aerosols (SSAs) are mainly produced by air bubbles bursting at the surface of the ocean as a result of wind stress (Jaegle *et al*., 2011). As the bubbles come back to the surface from whitecaps and burst, they lead to the injection of seawater film and jet drops into the atmosphere (Jaegle *et al*., 2011). SSAs are most dominant in the coastal parts of SA (see Figure 4d). A high aerosol loading (AOD ~ 0.065) of SSAs is observed at the southeastern coast in close proximity to the Indian Ocean. This high SSA loading could result from higher water temperature in the Indian Ocean compared to that of the Atlantic Ocean. This is supported by Grythe *et al*. (2014) who reported that temperature influences the production of SSAs, i.e. production of marine aerosols is favoured by higher water temperatures relative to lower ones. This is the reason for the observed moderate marine aerosol loading (AOD ~ 0.045) over the south coast and southwestern coast. Low SSA loading (AOD ~ 0.01) is observed in the interior of SA as would be expected.

4.4 | Seasonal BC, sulphate, dust and sea-salt AOD observed by MERRA-2

4.4.1 | Seasonal BC AOD

The seasonal spatial distribution of BC aerosols in SA averaged for the period 2004–2014 and retrieved by MERRA-2 is shown in Figure 5(a–d). The spring has the maximum BC AOD in a year followed by the winter. The summer and autumn are of lower and lowest BC AOD in the year. During summer (December, January, February) elevated aerosol loading (AOD ~ 0.008) is observed in the northern and southeastern parts of the country (see Figure 5a) while moderate BC aerosols (AOD ~ 0.0045) are observed in the interior and southern parts of SA. Lower BC aerosol loadings (AOD ~ 0.003) are observed in the southwestern parts of the country.

During autumn (March, April, May) elevated aerosol levels in the northern regions of SA close to the Botswana border are observed (see Figure 5b). The southeastern part of SA as well as Swaziland show an elevated aerosol loading compared to the rest of the country. The interior part of the country shows moderate aerosol loading (AOD ~ 0.0045) and lower aerosol loading is observed in the western parts of SA. Autumn shows the lowest aerosol loading compared to

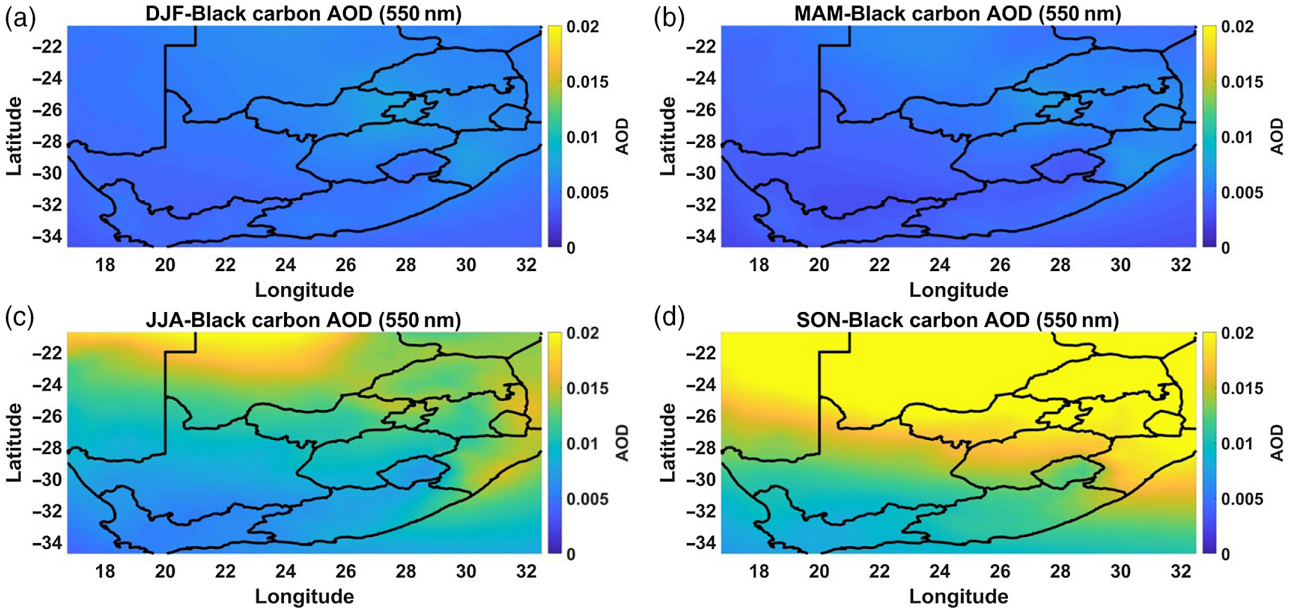

FIGURE 5 Seasonal variation of black carbon aerosol optical depth (AOD) (550 nm) for (a) summer, (b) autumn, (c) winter and (d) spring derived from Modern-Era Retrospective Analysis for Research and Applications, Version 2 (MERRA-2) data [Colour figure can be viewed at wileyonlinelibrary.com]

the other seasons. As stated earlier, the major BC contribution is from biomass burning which is transported to SA. The two reasons for the low BC aerosol concentration could be (a) that biomass burning occurs between late winter and late spring and (b) that the wind gusts are lower and the wind direction does not reach most of the interior of the country. Kruger *et al*. (2016) showed that the autumn has less strong wind gusts in the northeastern and northwestern regions. This implies that less BC aerosols travel to these regions and this could affect the BC concentration during this season.

During winter (June, July, August) an increase in aerosol loading is observed throughout the country (see Figure 5c). However, the southwestern parts of SA still show the lowest aerosol loading (AOD ~ 0.0045) compared to the rest of the country.

The highest BC aerosol loading in the country is observed in spring (September, October, November) and corresponds to AOD ~ 0.02 (see Figure 5d). Tesfaye *et al*. (2014) also reported elevated values of AOD in the spring on the eastern part of Limpopo. The SAFARI 2000 campaign showed that biomass burning during the spring from the neighbouring countries was responsible for the influx of BC aerosols into the eastern parts of Limpopo (Eck *et al*., 2003; Swap *et al*., 2003; Magi *et al*., 2009).

4.4.2 | Seasonal sulphate AOD

The seasonal spatial distribution of sulphate aerosols for SA, averaged from 2004 to 2014 and retrieved by MERRA-2, is shown in Figure 6(a–d). For the four seasons, elevated aerosol loading is always observed in the eastern part of the country, the Mpumalanga and Gauteng provinces. Lower aerosol loading is always observed in the interior and western parts of the country. Of the four seasons, summer shows the highest sulphate aerosol loading overall (AOD ~ 0.16) in the eastern parts of SA (see Figure 6a). Aurela *et al*. (2016) also reported on the dominance of sulphate aerosols in summer. Since sulphate aerosols emanate mostly from anthropogenic sources, Aurela *et al*. (2016) attributed the high sulphate loading to air masses that passed over the coal fired power station in Waterberg (23.6686 ° S, 27.6117 ° E), or the platinum group metal smelter in the Northam and Thabazimbi area (24.5828 ° S, 27.4028 ° E) may enhance the sulphate concentration by 14 or 37 times. This is just one study conducted by Aurela *et al*. (2016) for a power station located in the northwest province. However, all coal fired power stations would contribute to the high sulphate aerosol loading.

During winter, the AOD shows a lowest aerosol loading (AOD ~ 0.05) in the eastern parts of SA (see Figure 6c). The western parts of SA have a wet winter whereas eastern and interior parts of SA have a dry winter. Tesfaye *et al*. (2011) showed that there is a decrease in wind speed and Ångström exponent in SA over the winter. They further showed that the lower AOD during winter in the eastern and interior parts of SA is due to a low wind speed which results in less aerosol generation and dispersion. This is one of the reasons why lower sulphate aerosols are observed. Overall, factors such as meteorological conditions, prevailing winds, temperature changes, less precipitation and different oxidation rates experienced during summer and winter have an impact on the variation of sulphate concentration seasonally. Autumn and spring (see Figure 6b,d), on the other hand, show sulphate aerosol loadings of AOD ~0.1 and AOD ~0.11 respectively in the eastern parts of SA.

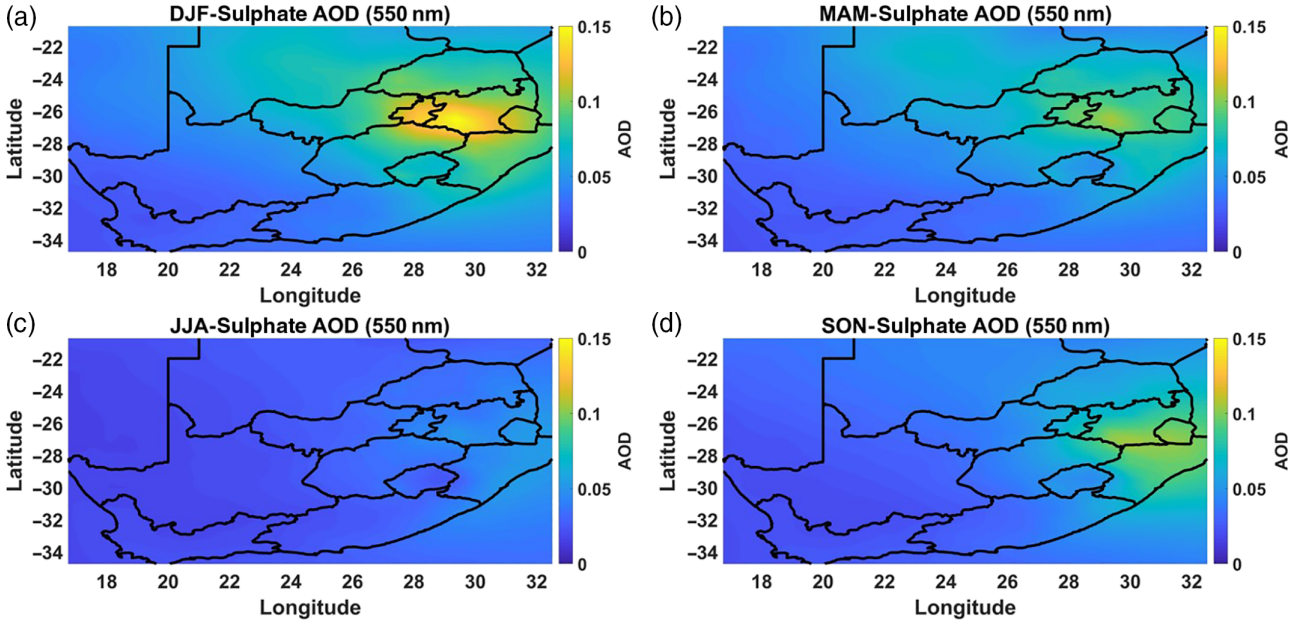

FIGURE 6 Seasonal variation of sulphate aerosol optical depth (AOD) (550 nm) for (a) summer, (b) autumn, (c) winter and (d) spring derived from Modern-Era Retrospective Analysis for Research and Applications, Version 2 (MERRA-2) data [Colour figure can be viewed at wileyonlinelibrary.com]

4.4.3 | Seasonal dust AOD

The seasonal spatial distribution of dust aerosols in SA, averaged from 2004 to 2014 and retrieved by MERRA-2, is shown in Figure 7(a–d). In all seasons, dust aerosols are predominantly observed in the northwestern parts of SA while lower aerosol loadings can be observed in the eastern parts of SA. Summer is the season with the highest dust aerosol loading (AOD ~ 0.01) with maximum concentrations observed in the northwestern parts of the country (see Figure 7a) corresponding to the Northern Cape province. The dust aerosols appear to originate from Namibia which borders SA, a finding supported by Tesfaye *et al.* (2015). Their study showed that the Kalahari and Namib Deserts were the main source for the detection of desert dust particles in the western parts of SA. During summer, moderate aerosol loading (AOD ~ 0.006) is observed in the central interior and south of the country. During autumn and winter mostly SA has low dust aerosol levels (AOD ~ 0.006) except for the northwestern regions which have moderate dust aerosol levels (see Figure 7b,c respectively). A change in wind

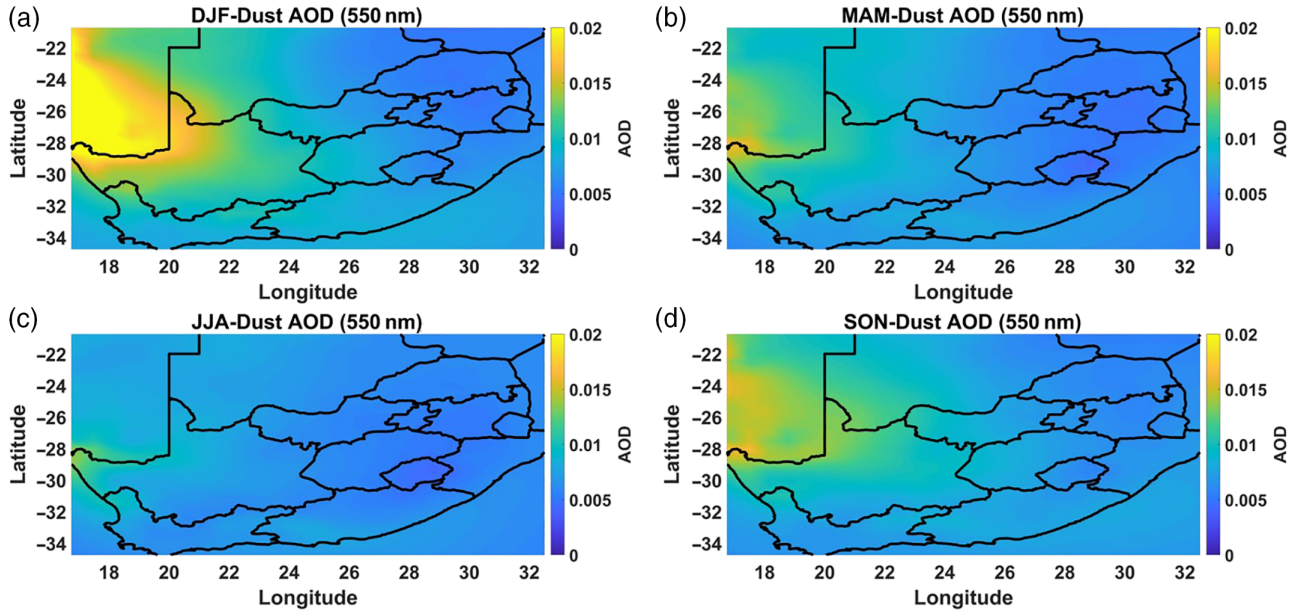

FIGURE 7 Seasonal variation of dust aerosol optical depth (AOD) (550 nm) for (a) summer, (b) autumn, (c) winter and (d) spring derived from Modern-Era Retrospective Analysis for Research and Applications, Version 2 (MERRA-2) data [Colour figure can be viewed at wileyonlinelibrary.com]

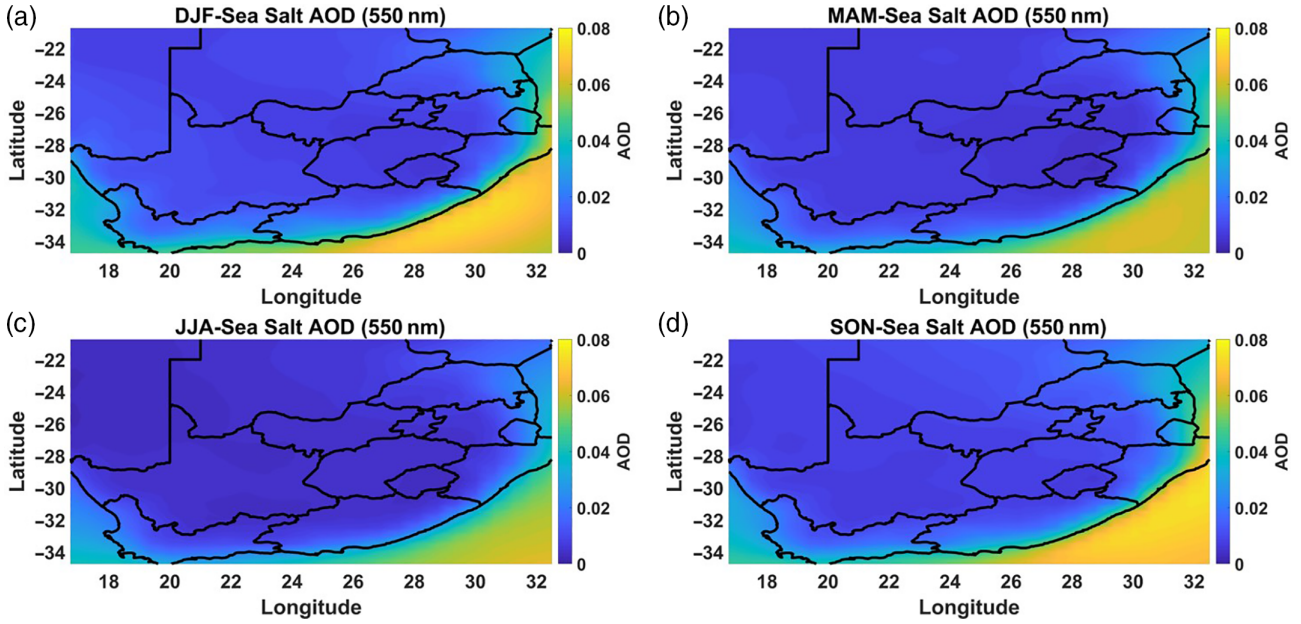

FIGURE 8 Seasonal variation of sea-salt aerosol optical depth (AOD) (550 nm) for (a) summer, (b) autumn, (c) winter and (d) spring derived from Modern-Era Retrospective Analysis for Research and Applications, Version 2 (MERRA-2) data [Colour figure can be viewed at wileyonlinelibrary.com]

direction with change in season might be the cause for the observed low aerosol loading. In spring (see Figure 7d) an increase in dust aerosol loading is seen. Namibia is the major source of dust aerosols and these aerosols are transported to SA in the northwestern parts to the interior of the country. In their study, Hersey *et al*. (2015) observed high dust aerosols using the GOCART model. They attributed this to be from windblown dust from the nearby Namib Desert.

4.4.4 | Seasonal marine AOD

The seasonal spatial distribution of SSAs in SA averaged from 2004 to 2014 and retrieved by MERRA-2 is shown in Figure 8(a–d). High SSA loading (AOD ~ 0.065) is observed in coastal areas in all seasons. The Indian Ocean has a higher SSA loading than the Atlantic Ocean in all seasons. The highest SSA loading in the Indian Ocean is observed in summer and spring (see Figure 8a,d). These seasons coincide with warmer water temperatures compared to autumn and winter; such conditions favour the production of marine aerosols (Grythe *et al*., 2014). During summer and spring (see Figure 8a,d) moderate SSAs (AOD ~ 0.01) are observed in the southwestern and northern parts of SA. Lower marine aerosol loading (AOD ~ 0.003) is observed in the interior of SA. For autumn and winter low marine aerosol loading is observed in the interior (see Figure 8b,c). By comparison, the northeastern parts of the country show moderate SSA loading (AOD ~ 0.025).

4.5 | GOCART natural and anthropogenic aerosols

In this investigation the GOCART model V006 product is used for the period January 1, 2000–December 31, 2007. There are no data after December 2007. The reason for using data from 2004 to 2007 is that this period falls within the period of the 10 year (2004–2014) trend studies carried out using MERRA-2 data. Figure 9 illustrates GOCART model results from July 2004 to December 2007 for the regional AOD trends from natural sources dust and anthropogenic sources BC and sulphates for the locations of Lephalale, Bloemhof, Mafikeng, Potchefstroom, Rustenburg and Vryburg. In each of these towns, it is observed from the modelled results that sulphates are the dominant contributing factor towards total anthropogenic AOD compared with the contributions due to dust and BC. In all locations, sulphate AOD levels show a very similar pattern of variation during the period from 2004 to 2007. However, the trend for 2004–2007 in all locations shows marked seasonal changes in sulphate AOD with highest values observed in February (summer) and lowest values observed in June (winter). The photochemical oxidation of SO_2 to sulphate in the summer could be the reason for the high calculated AOD values (De Meij *et al*., 2012). The atmospheric rate of oxidation of SO_2 increases with increasing relative humidity (Khoder, 2002) and since the relative humidity is high in summer for SA (Orimoloye *et al*., 2018) this favours the production of sulphate aerosols.

Consideration of BC shows that in all locations the variation is found to be similar for the period from July 2004 to December 2007. In all towns, August and September typically show the highest AOD corresponding to ~0.02. It is estimated to be due to biomass burning which begins in the late winter and early spring.

A high dust AOD is also observed in September of every year in all the towns. The results are found to be consistent with earlier findings by Tesfaye *et al*. (2015). Some of the attributions of dust particles are from the Namib and Kalahari Deserts.

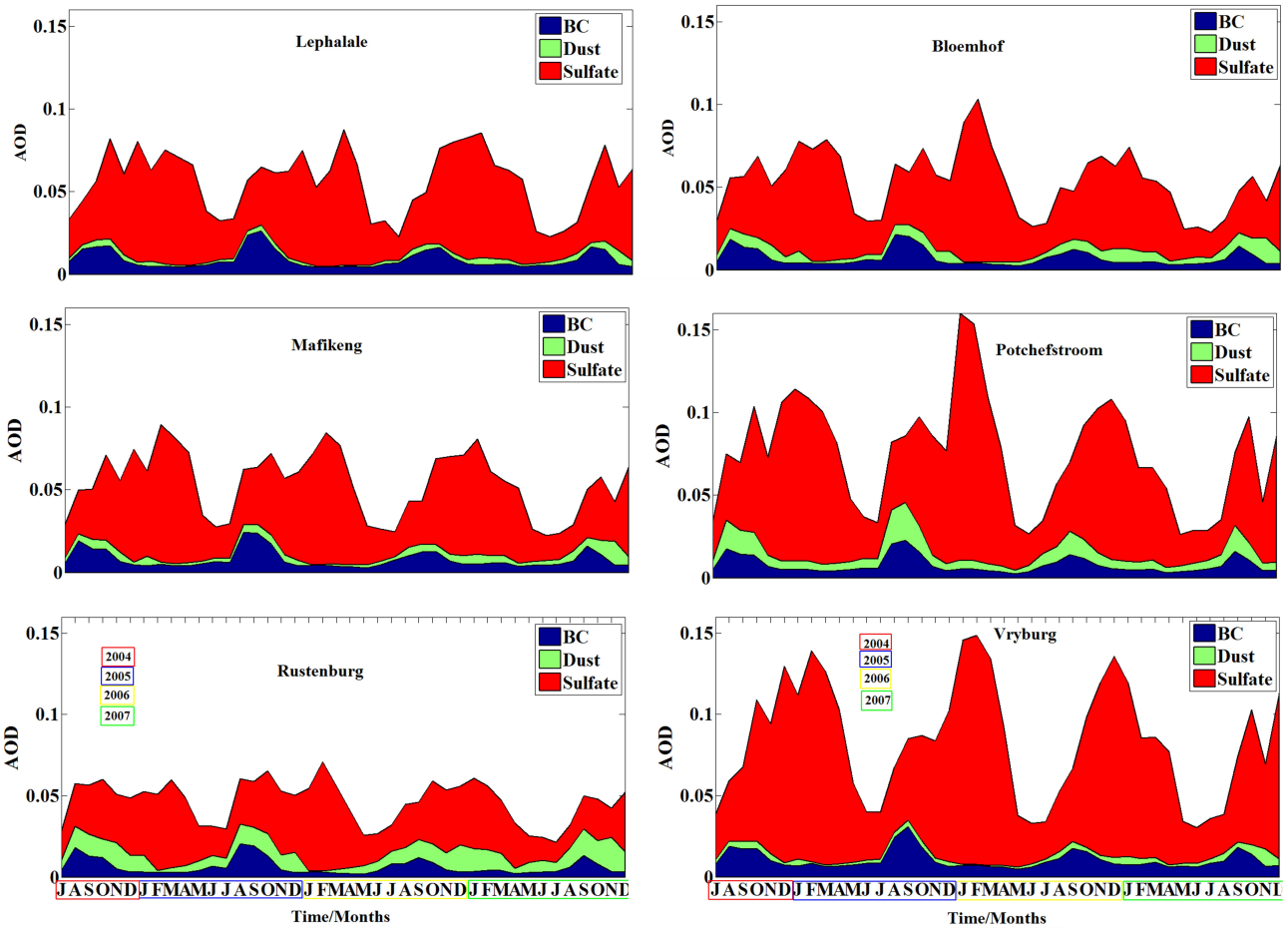

FIGURE 9 Estimated aerosol optical depth (AOD) trends for black carbon (BC), dust and sulphate aerosols in each region using the Goddard Chemistry Aerosol Radiation and Transport model from July 2004 to December 2007 [Colour figure can be viewed at wileyonlinelibrary.com]

4.6 | Case study in Lephalale

4.6.1 | CSIR mobile LIDAR

The vertical distributions of aerosol extinction co-efficient profiles are shown in Figure 10. These profiles were recorded at ~10:00 a.m. local time except for July 10, 2014, when it was recorded at 11:15 a.m. Similar profiles were observed on July 10, 13 and 16, 2014; however, the level at which the highest value of the extinction co-efficient occurs is different in the lower parts of the troposphere. The highest values of aerosol extinction co-efficients were observed at an altitude of about 20 m. These values are 0.244, 0.586 and 0.178/km respectively for the 3 days mentioned above. Three layers of aerosol clouds were observed between altitudes of 0.8 and 1.4 km on July 11, 2014. The peaks of each aerosol cloud layer were observed at altitudes of 0.86, 1.24 and 1.36 km, with aerosol extinction co-efficient values of each peak at 0.000781, 0.00604 and 0.00886/km respectively. On July 12, 2014, a sharp peak at a height of 1.14 km corresponding to an aerosol layer was observed with an extinction co-efficient of 0.0182/km. A similar profile was observed on July 14 and 15, 2014, with multiple peaks observed corresponding to layers of aerosol. These aerosol layers were observed on the lower part of the troposphere at ~1 km. A different type of profile was observed on July 17, 2014. Although the height profile shows a decrease in aerosol loading with increasing altitude, aerosol layers were observed at altitudes as low as 0.3 km. Multiple layers were also observed at altitudes less than 1 km. The results suggest that there was an overloading of aerosols in the lower part of the atmosphere during this period. From Figure 10, it can be seen that all profiles showed the existence of aerosols in the lower part of the atmosphere; however, aerosol levels decrease with increasing altitude.

4.6.2 | Comparison of CSIR LIDAR and CALIPSO extinction co-efficients

The range of the aerosol extinction co-efficient values observed for the 4 days (a) by CALIPSO was 0.01–0.34/km and (b) by CSIR mobile LIDAR was 0.07–0.58/km (see Table 2). As an example, the overpass time for July 16, 2014, was 1209 UTC with the closest daytime overpass distance 95 km. The overpass time for July 14, 2014, was 1222 UTC with closest daytime overpass distance 410 km. It is observed that the further the CALIPSO satellite is from the study site, the more the disagreement between the CSIR LIDAR and CALIPSO. There are several reasons for the observed differences in the aerosol extinction co-efficient values which include (a) that the horizontal distance between

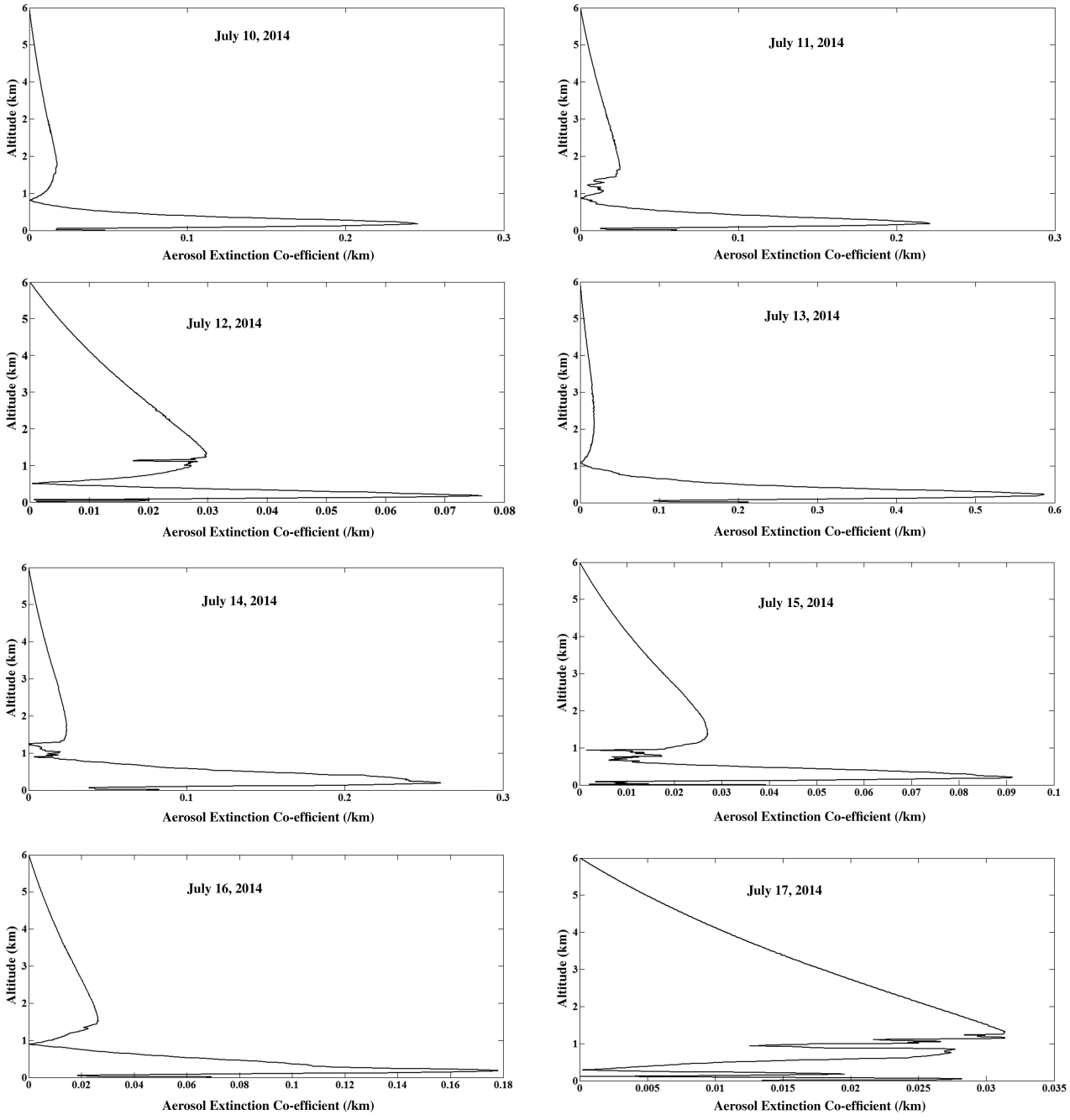

FIGURE 10 Vertical profile of aerosol extinction derived from Council for Scientific and Industrial Research (CSIR) mobile Light Detection and Ranging (LIDAR) signal returns recorded during July 2014 at Lephalale

TABLE 2 Comparison of aerosol extinction co-efficients using the CSIR mobile LIDAR and CALIPSO

Date (July 2014)	CSIR mobile LIDAR Aerosol extinction co-efficient (/km)	CALIPSO Aerosol extinction co-efficient (/km)
12	0.07	0.18
13	0.58	0.34
14	0.26	0.07
16	0.17	0.29

CALIPSO, Cloud-Aerosol LIDAR and Infrared Pathfinder Satellite Observations; CSIR, Council for Scientific and Industrial Research; LIDAR, Light Detection and Ranging.

CALIPSO and the CSIR mobile LIDAR site is as much as 150 km, (b) the retrieval algorithms differ and (c) the CSIR mobile LIDAR averages the data over a long period in a day whereas the CALIPSO satellite averages over a short period. Dust aerosols with extinction co-efficients in the range 0.01–0.38/km were observed by He and Yi (2014) in their studies over Wuhan (30.5 ° N, 114.4 ° E), China. Relating their study to what was observed in this work by the CSIR mobile LIDAR, dust aerosols were only observed on July 14 and 16, 2014, with extinction co-efficients of 0.26 and 0.17/km respectively.

5 | SUMMARY

Black carbon (BC) aerosols were observed to be dominant in the northeastern parts of South Africa (SA) while sulphate aerosols were observed to be dominant in eastern parts of the country. Dust aerosols were observed to be dominant in the northwestern parts of the country. Seasonal studies revealed that BC aerosols are more dominant in the eastern parts of SA during spring and less dominant in autumn. However, sulphate aerosols are more dominant in the eastern parts of SA during summer and less dominant in winter. This is consistent with what was reported by Kumar *et al.* (2014) who observed higher mean aerosol optical depth (AOD) during spring and summer. Dust aerosols are more dominant in the northwestern parts of SA during summer and less dominant in winter. This result agrees well with the findings from Tesfaye *et al.* (2015). Marine aerosols are more dominant in the coast area, the Indian Ocean and northeastern parts of SA during summer and winter, and less dominant during autumn and spring. Marine aerosol production is favoured by warm water.

The Goddard Chemistry Aerosol Radiation and Transport (GOCART) model was used from July 2004 to December 2007 to simulate AOD for sulphate, dust and BC tropospheric aerosols in six towns (Lephalale, Potchefstroom, Bloemhof, Mafikeng, Rustenburg and Vryburg) in SA. The model showed that sulphates contributed significantly in all the towns with BC also having some contribution. The GOCART model also indicated that there was no significant change in the sulphate aerosols during the period 2004–2007. The highest sulphate aerosol levels were modelled in the summer while the lowest sulphate aerosol levels were modelled in winter. The high sulphate concentration in summer is contributed to by an increase in relative humidity which favours the production of sulphates. The trends in BC aerosols revealed no change from 2004 to 2007. The highest BC aerosol levels were observed in August with the town of Lephalale showing the highest AOD. A high dust aerosol level was also observed during August in all locations.

Aerosol extinction co-efficient profiles were retrieved by the Council for Scientific and Industrial Research (CSIR) mobile Light Detection and Ranging (LIDAR) during the Lephalale campaign and were compared to aerosol extinction co-efficient profiles retrieved by Cloud-Aerosol LIDAR and Infrared Pathfinder Satellite Observations (CALIPSO). The aerosol extinction co-efficients between the CSIR LIDAR and CALIPSO were not in good agreement with each other for numerous reasons which include the difference in retrieval algorithms and that the horizontal distance between CSIR LIDAR and CALIPSO was about 150 km. However, aerosol extinction co-efficients of 0.26 and 0.17/km on July 14 and 16, 2014, respectively could be identified as dust aerosols.

ACKNOWLEDGEMENTS

We acknowledge the GES-DISC Interactive Online Visualization and Analysis Infrastructure (Giovanni) for providing us with MODIS, MISR and MERRA-2 data. CALIPSO data were obtained from the NASA Langley Research Centre Atmospheric Science Data Centre. We thank Mr Henk van Wyk and Ameeth Sharma for the technical work on the CSIR mobile LIDAR system. We thank Dr Steven Nkosi for his help with the LIDAR measurements in Lephalale.

REFERENCES

Ahmed, T., Dutkiewicz, V.A., Khan, A.J. and Husain, L. (2014) Long term trends in black carbon concentrations in the north eastern United States. *Atmospheric Research*, 137, 49–57.

Alexander, B., Park, R.J., Jacob, D.J., Li, Q.B., Yantosca, R.M., Savarino, J., Lee, C.C.W. and Thiemens, M.H. (2005) Sulfate formation in sea-salt aerosols: constraints from oxygen isotopes. *Journal of Geophysical Research*, 110, D10307.

Aurela, M., Beukes, J.P., Van Zyl, P., Vakkari, V., Teinilä, K., Saarikoski, S. and Laakso, L. (2016) The composition of ambient and fresh biomass burning aerosols at a savannah site, South Africa. *South African Journal of Science*, 112, 8.

Baddock, M.C., Bullard, J.E. and Bryant, R.G. (2009) Dust source identification using MODIS: a comparison of techniques applied to the Lake Eyre Basin, Australia. *Remote Sensing of Environment*, 113, 1511–1528.

Buchard, V., Randles, C.A., da Silva, A.M., Darmenov, A., Colarco, P.R., Govindaraju, R., Ferrare, R., Hair, J., Beyersdorf, A.J., Ziemba, L.D. and Yu, H. (2017) The MERRA-2 aerosol reanalysis, 1980 onward. Part II: Evaluation and case studies. *Journal of Climate*, 30, 6851–6872.

Cahoon, D.R., Jr., Stocks, B.J., Levine, J.S., Cofer, W.R., III and O'Neill, K. (1992) Seasonal distribution of African savanna fires. *Nature*, 359, 812–815.

Campbell, J.R., Welton, E.J., Spinhirne, J.D., Ji, Q., Tsay, S.-C., Piketh, S.J., Barenbrug, M. and Holben, B.N. (2003) Micropulse LIDAR observations of tropospheric aerosols over northeastern South Africa during the ARREX and SAFARI 2000 dry season experiments. *Journal of Geophysical Research*, 108, 8497.

Cheng, T., Chen, H., Gu, X., Yu, T., Guo, J. and Guo, H. (2012) The inter-comparison of MODIS, MISR and GOCART aerosol products against AERONET data over China. *Journal of Quantitative Spectroscopy and Radiative Transfer*, 113, 2135–2145.

Chin, M., Ginoux, P., Kinne, S., Torres, O., Holben, B.N., Duncan, B.N., Martin, R.V., Logan, J.A., Higurashi, A. and Nakajima, T. (2001) Tropospheric aerosol optical thickness from the GOCART model and comparisons with satellite and Sun photometer measurements. *Journal of the Atmospheric Sciences*, 59, 461–483.

Chin, M., Rood, R.B., Lin, S.J., Muller, J.F. and Thompson, A.M. (2000) Atmospheric sulfur cycle simulated in the global model GOCART': model description and global properties. *Journal of Geophysical Research*, 105, 671–687.

Cooke, W.F. and Wilson, J.J. (1996) A global black carbon aerosol model. *Journal of Geophysical Research-Atmospheres (1984–2012)*, 101, 19395–19409.

De Meij, A., Pozzer, A. and Lelieveld, J. (2012) Trend analysis in aerosol optical depths and pollutant emission estimates between 2000 and 2009. *Atmospheric Environment*, 51, 75–85.

Diner, D.J., Beckert, J.C., Reilly, T.H., Bruegge, C.J., Conel, J.E., Kahn, R.A., Martonchik, J.V., Ackerman, P.T., Davies, R., Gerstl, S.A.W., Gordon, H. R., Muller, J.P., Myneni, R.B., Sellers, P.J., Pinty, B. and Verstraete, M.M. (1998) Multi-angle Imaging SpectroRadiometer (MISR) instrument description and experiment overview. *IEEE Transactions on Geoscience and Remote Sensing*, 36, 1072–1087.

Eck, T.F., Holben, B.N., Ward, D.E., Mukelabai, M.M., Dubovik, O., Smirnov, A., Schafer, J.S., Hsu, N.C., Piketh, S.J., Queface, A., Roux, J.L., Swap, R.J. and Slutsker, I. (2003) Variability of biomass burning aerosol optical characteristics in southern Africa during the SAFARI 2000 dry season campaign and a comparison of single scattering albedo estimates from radiometric measurements. *Journal of Geophysical Research*, 108, 8477.

El-Metwally, M., Alfaro, S.C., Abdel Wahab, M.M., Zakey, A.S. and Chatenet, B. (2010) Seasonal and inter-annual variability of the aerosol content in Cairo (Egypt) as deduced from the comparison of MODIS aerosol retrievals with direct AERONET measurements. *Atmospheric Research*, 97, 14–25.

Formenti, P., Elbert, W., Maenhaut, W., Haywood, J., Osborne, S. and Andreae, M.O. (2003) Inorganic and carbonaceous aerosols during the Southern African Regional Science Initiative (SAFARI 2000) experiment:

chemical characteristics, physical properties, and emission data for smoke from African biomass burning. *Journal of Geophysical Research*, 108, 8488.

Freiman, M.T. and Piketh, S.J. (2003) Air transport into and out of the industrial Highveld region of South Africa. *Journal of Applied Meteorology*, 42, 994–1002.

Ginoux, P., Chin, M., Tegen, I., Prospero, J.M., Holben, B., Dubovik, O. and Line, S.-L. (2001) Sources and distributions of dust aerosols simulated with the GOCART model. *Journal of Geophysical Research*, 106, 255–273.

Ginoux, P., Prospero, J.M., Torres, O. and Chin, M. (2004) Long-term simulation of global dust distribution with the GOCART model: correlation with North Atlantic Oscillation. *Environmental Modelling and Software*, 19, 113–128.

Grythe, H., Ström, J., Krejci, R., Quinn, P. and Stohl, A. (2014) A review of sea-spray aerosol source functions using a large global set of sea salt aerosol concentration measurements. *Atmospheric Chemistry and Physics*, 14, 1277–1297.

Guo, J., Gu, X., Yu, T., Cheng, T. and Chen, H. (2014). Trend analysis of the aerosol optical depth from fusion of MISR and MODIS retrievals over China. *IOP Conference Series: Earth and Environmental Science* 17, 012036.

He, Y. and Yi, F. (2014) Dust aerosols detected using a ground-based polarization LIDAR and CALIPSO over Wuhan (30.5°N, 114.4°E), China. *Advances in Meteorology*, 2015, 18.

Hersey, S.P., Garland, R.M., Crosbie, E., Shingler, T., Sorooshian, A., Piketh, S. and Burger, R. (2015) An overview of regional and local characteristics of aerosols in South Africa using satellite, ground, and modeling data. *Atmospheric Chemistry and Physics*, 15, 4259–4278.

Jaegle, L., Quinn, P.K., Bates, T.S., Alexander, B. and Lin, J.-T. (2011) Global distribution of sea salt aerosols: new constraints from *in situ* and remote sensing observations. *Atmospheric Chemistry and Physics*, 11, 3137–3157.

Kaskaoutis, D.G., Kambezidisa, H.D., Adamopoulos, A.D. and Kassomenos, P. A. (2006) Comparison between experimental data and modeling estimates of aerosol optical depth over Athens, Greece. *Journal of Atmospheric and Solar - Terrestrial Physics*, 68, 167–1178.

Khoder, M.I. (2002) Atmospheric conversion of sulfur dioxide to particulate sulfate and nitrogen dioxide to particulate nitrate and gaseous nitric acid in an urban area. *Chemosphere*, 49, 675–684.

Kneen, M.A., Lary, D.J., Harrison, W.A., Annegarn, H.J. and Brikowski, T.H. (2016) Interpretation of satellite retrievals of PM2.5 over the southern African interior. *Atmospheric Environment*, 128, 53–64.

Kompalli, S.K., Babu, S.S., Moorthy, K.K., Manoj, M.R., Kumar, N.V.P., Shae, K.H.B. and Joshi, A.K. (2014) Aerosol black carbon characteristics over Central India: temporal variation and its dependence on mixed layer height. *Atmospheric Research*, 147–148, 27–37.

Kruger, A.C., Pillay, D.L. and van Staden, M. (2016) Indicative hazard profile for strong winds in South Africa. *South African Journal of Science*, 112, 1–11.

Kuik, F., Lauer, A., Beukes, J.P., Van Zyl, P.G., Josipovic, M., Vakkari, V., Laakso, L. and Feig, G.T. (2015) The anthropogenic contribution to atmospheric black carbon concentrations in southern Africa: a WRF-Chem modeling study. *Atmospheric Chemistry and Physics*, 15, 8809–8830.

Kumar, K.R., Sivakumar, V., Yin, Y., Reddy, R., Kang, N., Diao, Y., Adesina, A.J. and Yu, X. (2014) Long-term (2003–2013) climatological trends and variations in aerosol optical parameters retrieved from MODIS over three stations in South Africa. *Atmospheric Environment*, 95, 400–408.

Lopes, F.G.S., Mariano, G.L., Landulfo, E. and Mariano, E.V.C. (2012) Impacts of biomass burning in the atmosphere of the south eastern region of Brazil using remote sensing systems. In: Abdul-Razzak, H. (Ed.) *Atmospheric Aerosols - Regional Characteristics – Chemistry and Physics* Intech, pp. 247–272.

Magi, B.I. (2009) Chemical apportionment of southern African aerosol mass and optical depth. *Atmospheric Chemistry and Physics*, 9, 7643–7655.

Magi, B.I., Ginoux, P., Ming, Y. and Ramaswamy, V. (2009) Evaluation of tropical and extratropical Southern Hemisphere African aerosol properties simulated by a climate model. *Journal of Geophysical Research*, 114, D14204.

Orimoloye, I.R., Mazinyo, S.P., Nel, W. and Iortyom, E.T. (2018) Assessing changes in climate variability observation and simulation of temperature and relative humidity: a case of East London, South Africa. *Research Journal of Environmental Sciences*, 12, 1–13.

Panicker, A.S., Pandithurai, G., Safai, P.D., Dipu, S., Prabha, T.V. and Konwar, M. (2014) Observations of black carbon induced semi direct effect over northeast India. *Atmospheric Environment*, 98, 685–692.

Piketh, S.J., Annegarn, H.J. and Tyson, P.D. (1999) Lower tropospheric aerosol loadings over South Africa: the relative contribution of aeolian dust, industrial emissions and biomass burning. *Journal of Geophysical Research*, 104, 1597–1607.

Queface, A.J., Piketh, S.J., Eck, T.F., Tsay, S.-C. and Mavume, A.F. (2001) Climatology of aerosol optical properties in Southern Africa. *Atmospheric Environment*, 45, 2910–2921.

Randles, C.A., da Silva, A.M., Buchard, V., Colarco, P.R., Darmenov, A., Govindaraju, R., Smirnov, A., Holben, B., Ferrare, R., Hair, J., Shinozuka, Y. and Flynn, C.J. (2017) The MERRA-2 aerosol reanalysis, 1980 onward. Part I: System description and data assimilation evaluation. *Journal of Climate*, 30, 6823–6850.

Ray, S. and Kim, K.-H. (2014) The pollution status of sulfur dioxide in major urban areas of Korea between 1989 and 2010. *Atmospheric Research*, 147–148, 101–110.

Rienecker, M.M., Suarez, M.J., Gelaro, R., Todling, R., Bacmeister, J., Liu, E., Bosilovich, M., Schubert, S., Takacs, L., Kim, G.-K., Bloom, S., Chen, J., Collins, D., Conaty, A., Da silva, A., Joiner, J., Koster, R.D., Lucchesi, R., Molod, A., Owens, T., Pawson, S., Pegion, P., Redder, C., Reichle, R., Robertson, F., Ruddick, A.G., Sienkiewicz, M. and Woollen, J. (2011) MERRA: NASA's modern-era retrospective analysis for research and applications. *Journal of Climate*, 24, 3624–3648.

Ross, K.E., Piketh, S.J., Bruintjes, R.T., Burger, R.P., Swap, R.J. and Annegarn, H.J. (2003) Spatial and seasonal variation in CCN distribution and the aerosol–CCM relationship over southern Africa. *Journal of Geophysical Research*, 108, 8481.

Seinfeld, J.H. and Pandis, S.N. (2006) *Atmospheric Chemistry and Physics: From Air Pollution to Climate Change*, 2nd edition. New York, NY: John Wiley & Sons.

Sharma, A., Sivakumar, V., Bollig, C., van der Westhuizen, C. and Moema, D. (2009) System description of the mobile LIDAR of the CSIR, South Africa. *South African Journal of Science*, 105, 456–462.

Shikwambana, L. and Sivakumar, V. (2016) Observation of clouds using the CSIR transportable LIDAR: a case study over Durban, South Africa. *Advances in Meteorology*, 2016, 9.

Sivakumar, V., Tesfaye, M., Alemu, W., Moema, D., Sharma, A., Bollig, C. and Mengistu, G. (2009) CSIR South Africa mobile LIDAR – first scientific results: comparison with satellite, sun photometer and model simulations. *South African Journal of Science*, 105, 449–455.

Swap, R.J., Annegarn, H.J., Suttles, J.T., King, M.D., Platnick, S., Privette, J.L. and Scholes, R.J. (2003) Africa burning: a thematic analysis of the Southern African Regional Science Initiative (SAFARI 2000). *Journal of Geophysical Research*, 108, 8465.

Tesfaye, M., Botai, J., Sivakumar, V. and Tsidu, G.M. (2014) Simulation of biomass burning aerosols mass distributions and their direct and semi-direct effects over South Africa using a regional climate model. *Meteorology and Atmospheric Physics*, 125, 177–195.

Tesfaye, M., Sivakumar, V., Botai, J. and Mengistu Tsidu, G. (2011) Aerosol climatology over South Africa based on 10 years of Multiangle Imaging Spectroradiometer (MISR) data, *Journal of Geophysical Research*, 116, D20216.

Tesfaye, M., Tsidu, G.M., Botai, J., Sivakumar, V. and de W Rautenbach, C.J. (2015) Mineral dust aerosol distributions, its direct and semi-direct effects over South Africa based on regional climate model simulation. *Journal of Arid Environments*, 114, 22–40.

Winkler, W., Formenti, P., Esterhuyse, D.J., Swap, R.J., Helas, G., Annegarn, H. J. and Andreae, M.O. (2008) Evidence for large-scale transport of biomass burning aerosols from Sun photometry at a remote South African site. *Atmospheric Environment*, 42, 5569–5578.

Zhang, X., Rao, R., Huang, Y., Mao, M., Berg, M.J. and Sun, W. (2015) Black carbon aerosols in urban central China. *Journal of Quantitative Spectroscopy and Radiative Transfer*, 150, 3–11.

Zunckel, M., Robertson, L., Tyson, P.D. and Rodhe, H. (2000) Modelled transport and deposition of sulphur over southern Africa. *Atmospheric Environment*, 34, 2797–2808.

How to cite this article: Shikwambana L, Sivakumar V. Investigation of various aerosols over different locations in South Africa using satellite, model simulations and LIDAR. *Meteorol Appl*. 2019; 26:275–287. https://doi.org/10.1002/met.1761